

RADIATION PROTECTION PROBLEMS AT THE STANFORD TWO MILE LINEAR ACCELERATOR*

T. M. Jenkins, Richard C. McCall and Gary J. Warren

Stanford Linear Accelerator Center, Stanford University, Stanford, California

INTRODUCTION

The Stanford two mile long accelerator is a 20 GeV linear electron accelerator scheduled for completion in mid-1966. The machine, with its shielding, is designed for an eventual beam current of 60 μ a at 40 BeV, which is 2.4 MW of beam power. The accelerator site is located in rolling hills with the project boundary at least 500 feet from any point likely to be struck by the beam; the resulting decrease in radiation level at the boundary is such that shielding considerations for radiation workers inside, and the general population outside the boundary yield essentially the same requirements for shielding thickness. This accelerator has many problems that are typical of any high energy accelerator and some that are peculiar to the type of accelerator it is, and to its sometimes unique design.

This paper will attempt to delineate some of the problems at SLAC, and their solutions, as well as spell out areas of agreement or disagreement with a few of the early shielding calculations that were used on the initial design of the machine.

GENERAL

The accelerator complex may be divided into three separate parts which have different radiation problems deriving, in part, from their different functions. For example, the straight ahead shielding may be dominated by μ mesons which would be important for target areas. The three parts are: 1) the accelerator part itself, a two mile long disk-loaded waveguide about four inches in diameter located in a housing under 25 feet of earth. Above this is a gallery housing the S-band klystrons; 2) the beam switchyard, where the electron beam will be deflected to the various experimental areas; and 3) the target areas themselves. See Figure 1.

Of these three parts, only the accelerator structure, with its associated klystron gallery, is near operational status. The first 660 feet have been operated with injector and target at about 1.5 GeV and 5 kW beam power. This paper discusses primarily the accelerator tunnel, as it is only there that we have made any measurements.

Figure 2 shows a cross-sectional view of the accelerator looking east in the direction of the beam. In this figure we may indicate many of the problem areas encountered at SLAC as well as give a general cross-sectional view of the accelerator. The klystron gallery is separated from the accelerator housing by 25 feet of earth. This separation allows for easy maintenance of klystrons and their associated electronics; however, other problems are created. Every 20 feet there is a 27 inch diameter service penetration for vacuum, rf, water lines, and so on. These are potential sources of radiation. At each of the 30 sectors there is a man accessway which is a 30 inch diameter pipe. Both 27 inch diameter

*Work supported by U. S. Atomic Energy Commission.

service penetration and man accessway must be air sealed to keep radioactive air inside. In addition, there are seven equipment accessways which must be sealed and shielded. (Note that the radiation measurements or calculations inside the accelerator housing, or shafts, must account for the effect of ducting.)

Radiation problems may be grouped into three divisions: 1) prompt radiation from the accelerator; 2) residual radiation of accelerator parts; and 3) radiation not associated with the beam.

1. Prompt Radiation from the Accelerator

- A. Radiation levels at the shield surface. Radiation levels at the surface of the 25 foot earth shield have been calculated by H. DeStaebler¹ in SLAC Report No. 9 where high energy neutrons dominate the shielding calculations. He used the following formulae:

The yield of secondary neutrons per incident electron of energy E_0 is

$$\frac{d^2n}{dTd\Omega} = \left(0.57 \frac{E_0 X_0}{k^2} \right) \frac{N_0}{A} \left[KA \frac{d\sigma}{d\Omega^*} \right] \frac{\partial(k, \theta^*)}{\partial(T, \theta)} \quad (*\text{denotes c.m. system})$$

where the first term in the expression is the differential photon track length as derived under approximation A of shower theory, the bracketed term is the cross section per nucleus as given in the c.m. system, and the last term is the Jacobian which converts from the c.m. to lab system. The dose of neutrons at the surface of the shield was then solved in two ways. First using a method due to Moyer,² DeStaebler calculates

$$\text{Dose (mrem/hr)} = 3.6 \times 10^6 f \frac{I_f E_f < F'B >}{L R + H} \int_{-\pi/2}^{\pi/2} d\theta \int_0^{\infty} dT \frac{1}{e} \frac{d^2n}{dTd\Omega} \exp - H/[\lambda(T) \sin \theta]$$

where

f = fraction of beam power absorbed

$I_f E_f$ = total beam power (2.4 MW)

L = length of machine (10^4 feet)

$< F'B >$ = RBE dose per neutron flux (1.25×10^{-7} rem/n-cm²)

R = radius of tunnel (≈ 5 feet)

H = thickness of shield surrounding the accelerator (in cm)

θ = angle of neutron emission with respect to beam direction (in radians)

T = energy of neutrons emitted from machine
 $\frac{d^2n}{dTd\Omega}$ = neutron yield per absorbed electron of energy (n/MeV-sr)
 ϵ = final beam energy (45 BeV)
 $\lambda(T)$ = removal mean free path of neutrons of energy T ; approximately
 170 g/cm² at large angles

The dose rate was also obtained by solving three coupled integro-differential equations describing the transport of neutrons, protons and charged pions on a computer for the Princeton group by ORNL. Both methods give essentially the same results. DeStaebler shows Figure 3 for the dose rate at the surface of a 25 foot shield as a function of the length over which the power is uniformly absorbed. The radiation levels at the surface of the shield are due to incident neutrons in the 300-500 MeV range. Levels are proportional to the amount of beam power absorbed, so we may scale the figure accordingly. Figure 3 estimates the level at the surface of the shield for 2.4 MW absorbed in a point to be 60 mrem/hr. For the same conditions the level at the project boundary would be 0.2 mrem/hr. This is a somewhat unlikely occurrence as there are various safeguards to assure that the machine power goes where it is directed, i.e., to a target or beam dump. A more reasonable estimate, based partly on experience at the Stanford 1 BeV 330 foot accelerator, is that 3% or less of the final beam power might be lost in the two mile length of accelerator. The lower curve shows the level as derived from a uniform 3% beam power loss along the accelerator. For the same conditions, 3% beam loss at a point gives 1.8 mrem/hr at the shield surface, and 0.006 mrem/hr at the project boundary, which is essentially background.

To localize beam losses, and areas of residual radiation, beam scrapers have been placed at the end of each of the 30 sectors. Thus, we might figure, for ease of computation, that 1/30 of 3% to be absorbed in each scraper, or 2.4 kW. At the 660 foot portion of the accelerator now in operation, we beamed 2.7 kW (1.3 BeV) into a copper target simulating a typical beam scraper, and measured the neutron levels in the klystron gallery. These measurements are obscured by the presence of scattered neutrons coming from the penetrations nearby ('skyshine'). For 2.7 kW absorbed in a point, the radiation level at the surface of the shield is $60 \times 2.7/2.4 \times 10^3 = .067$ mrem/hr. This is roughly ten times background in the Palo Alto area; so 2.7 kW should show a measurable yield at the shield surface. The level measured at the shield surface 10 feet from a penetration (and almost directly over the target) was 1.3 mrem/hr; surrounding the detector by six inches of paraffin to eliminate air-scattered neutrons dropped the level to .13 mr/hr which is in close agreement with calculations. (Note: An average energy of ~ 1 MeV was assumed in converting measured neutron fluxes to dose rates.)

- B. Giant resonance neutrons. The prompt radiation from a scraper, target, etc., should be composed of high energy particles (neutrons, protons, mesons, etc.), γ 's and giant resonance neutrons. Giant resonance neutrons have figured greatly in the shielding calculations

at SLAC. For example, they are estimated to be the main source of neutron dose streaming up the penetrations.

The yield of giant resonance neutrons per incident electron of energy E_0 is given by³

$$n = \int 0.57 \frac{E_0}{k^2} X_0 \frac{N_0}{A} \sigma(k) dk$$

$$\approx 0.57 \frac{N_0}{A} X_0 \frac{E_0}{k_0^2} \int \sigma(k) dk \quad (\text{neutrons/electron})$$

where

k_0 = photon energy at peak of giant resonance

N_0 = Avogadro's number

A = atomic weight of target

X_0 = radiation length of target

$\sigma(k)$ = giant resonance cross section

The integrated cross section may be approximated by the dipole sum rule estimation

$$\int \sigma(k) dk \approx 60 \frac{Z(A-Z)}{A} \text{ MeV-mb}$$

or measured values used when available. The approximate yield of giant resonance neutrons per incident electron of energy $E_0 = 1 \text{ BeV}$ is then

$$n = 37 \frac{A - Z}{AZ \ln(183 Z^{-1/3})} \approx 1/5 \text{ neutron/BeV}$$

and for $P = EI = 1 \text{ MW}$, we get $Q = 1.25 \times 10^{15} \text{ neutrons/second-MW}$. This has been verified at high energies.^{4,5} It was checked by SLAC⁶ at energies of 38 MeV and 1.3 BeV using moderated indium foils. The value at 38 MeV was 0.2 n per BeV, and the measured value at 1.3 BeV was 80% of the calculated value, which was within the limits of that particular experiment.

The giant resonance neutron yield should be isotropic in the lab system. Measurements made by D. Neet⁷ at the Mark III electron accelerator, 990 MeV, with moderated indium foils and ion chambers show an approximate isotropic neutron yield, with a forward peaked γ yield. Measurements made in the tunnel at the 660 foot accelerator, 1.3 BeV, show an isotropic neutron flux and a forward peaked γ yield. The detector sensitivity drops for neutrons with energies greater than

14 MeV, so that it does not easily detect the high energy neutrons in the forward direction.

The γ/n dose ratio inside the accelerator tunnel has been estimated to lie somewhere between 10 and 1000.⁴ With an incident energy of 1.3 BeV, we measured γ/n ratios (which are a function of angle from the target) of between four and 14, using for our γ measurements LiF (TLD 700) thermoluminescent dosimeters. See Figure 4.

We note here that measurements of high energy neutrons in the presence of the intense γ fluxes are difficult due to competing photon induced reactions. For example, the well known C^{12} , $(n,2n)$ reaction to measure neutrons with $E > 20$ MeV ($\sigma \approx 22$ mb) must compete with the C^{12} (γ,n) reaction ($\sigma \approx 9$ mb).

- C. Radiation streaming up the penetrations. In general, the flux at a point in a duct (penetration) consists of a direct part which decreases like $1/z^2$ and a part that has scattered off the walls (depends upon albedo) and decreases faster than $1/z^2$. The fractional transmission, $g(z)$, is given by³

$$g(z) = \frac{\Phi(z)}{\Phi(o)} \approx \frac{a^2}{z^2} \left[1 + K \frac{a}{z} \right], \text{ for } 4 < z/a < 36,$$

where

a = radius of a cylindrical duct

K = 60 for γ 's and thermal neutrons, and more like 16 for fast neutrons

$\Phi(z)$ = flux at a point (z) in the duct

$\Phi(o)$ = flux at entrance

The fractional transmission has been measured for thermal neutrons by other authors⁶ and is shown in Figure 5 which was used in calculating dose at the top of our penetrations. PuBe neutrons closely followed the same curve when measured in a 27 inch diameter service penetration.

The original calculations of DeStaebler were made assuming a line source located 2'8" to the side and 5'4" under the roof near a penetration, and were given by⁵

$$D(\text{mrem/hr}) = 3.6 \times 10^6 F g(z) \Phi(o)$$

where

D = level in gallery

3.6×10^6 = factor which converts rem/sec to mrem/hr

F = biological effect per fast neutron (3.8×10^{-8} rem/n cm^{-2})

g = attenuation in duct; for $z/a = 21$ as in case of a service penetration, $g = 10^{-3}$ from Figure 5

$\varphi_{(o)}$ = fast neutron flux at the start of a penetration

At the 660 foot portion, we beamed into a target 17 feet from a penetration with 1.25 kW absorbed power. We calculate $\varphi_{(o)}$ to be 4.12×10^5 n/cm²-sec, and

$$D = (3.6 \times 10^6)(3.8 \times 10^{-8})(10^{-3})(4.12 \times 10^5) \\ = 55 \text{ mrem/hr}$$

The measured value is 60 mrem/hr for the above conditions, which is in excellent agreement with calculations.

For an assumed 3% uniform beam loss along the accelerator and 2.4 MW, DeStaebler calculates 68 mrem/hr in the klystron gallery from neutrons streaming up the service penetrations. Evidently some form of plugging is necessary; due to the various electrical service pipes, vacuum, and rf service, plugging is not an easy task. Our solution has been to place a wooden diaphragm 27 inches from the top with powdered serpentine rock high in water content poured into it, which may be removed with a vacuum cleaner. The mean free path for the penetration neutrons in serpentine was measured as 30 g/cm², about the same as fission neutrons in concrete. To achieve tolerance level (SLAC tolerance is 0.75 mrem/hr), we must have a transmission factor of about 10^{-3} , or a serpentine thickness of about 24 inches.

The levels at the tops of the other penetrations (man accessways and material accessways) have been calculated,⁸ again assuming a uniform 3% loss of 2.4 MW, to be 1 mrem/hr for the man accessways, and 165 mrem/hr for the equipment accessways. The addition of beam scrapers, which do not 'see' these entrances, should cut these values by at least a factor of 10. The equipment accessways are capped by three-foot thick concrete blocks which may be removed only with a crane.

No calculations were made for γ 's up the penetration, but they may be derived from $g(z) = (a/z)^2[1 + K a/z]$ with $K = 60$. We use the same value, $g(z) = 10^{-3}$. Then, knowing the γ/n dose ratio inside the tunnel as measured (we will use 5 which is the value near 90°) the dose at the top of the service penetration should be 275 mr/hr. We measure 300 mr/hr.

2. Residual Radiation of Accelerator Structures and Shielding

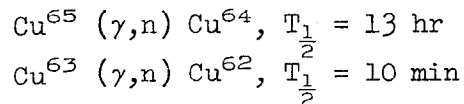
Beam loss along the accelerator is estimated to be 3% of the final beam power. This will occur primarily in the 30 beam scrapers and small couplings along the machine. There will be times, especially during tune-up, when local points will intercept more of the beam. An example of this was seen during initial operations on the 660 foot accelerator where, using moderated indium foils to measure the neutron flux, we noted an apparent beam power loss of 8.7% in the collimator at the end of sector 1.

The accelerator will be typical of our problems, with activation of metal parts, concrete in the walls, water and air. In concrete, the principal reaction we are concerned with is $\text{Na}^{23}(n,\gamma)\text{Na}^{24}$ with $T_{1/2} = 15$ hours.

In certain areas, activation of the concrete is a significant portion of the radiation inside the tunnel. Boron frit (B_2O_3) has been added to the concrete walls near the positron target and in the beam switchyard, and the effectiveness¹⁰ is shown in Figure 6. However, the neutron fluxes are likely to be too high also in the vicinity of the beam scrapers. Our approach to reduce the residual activity of the concrete is to clad each of the scrapers with a five inch thick jacket constructed either of borated paraffin or paraffin with a cadmium liner. Measurements⁶ made at 70 MeV, and with a PuBe source, indicate that such a jacket ten inches in diameter will reduce the concrete activity by a factor of ten. See Figure 7.

The residual radiation level from Cu^{64} at five feet distance from a beam scraper having absorbed 1 kW to saturation is calculated¹¹ to be 1.6 R/hr. A two inch thick Pb jacket has been designed to replace the boron-paraffin jacket during down times whenever personnel will be working nearby. This lead clamshell should reduce the radiation levels three feet away from a scraper that has absorbed 1 kW to saturation for Co^{60} to 10 mr/hr.

Along the accelerator waveguide, the principal reactions are



with Co^{58} ($T_{1/2} = 71d$) and Co^{60} ($T_{1/2} = 5.3 \text{ yr}$) becoming important daughter products after long irradiation times, and long ($> 100 \text{ hrs}$) waiting times. Calculations of residual activity are made from a modification of the yield formula¹² given previously,

$$R(\text{curies}) = 58 \text{ g} \left(\frac{X_0}{A} \right) \int \frac{\sigma dk}{k^2}$$

where

g = fractional atomic abundance of parent nuclide

X_0 = radiation length (g/cm^2)

A = atomic weight of material

$\sigma(k)$ = cross section in μbarns

Table 1 shows some of the radioactive products that will be formed from copper.

For a uniform 3% of 2.4 MW beam power loss along the accelerator, and 10^2 to 10^4 hours irradiation times, the levels inside the tunnel as a function of wait time are shown in Figure 8.

An ionization chamber lowered down various service penetrations gives a beam loss profile during machine operation of which Figure 9 is typical for this period of operation. This profile is a function of many variables, such as focusing, steering, phasing, and so on. Residual activity profiles follow the same shape, with the beam scrapers and small flexible couplings being the main hot spots. After absorbing 1 kW of beam power, levels two feet away from a target with two inches Pb shielding are typically a few R per hour five minutes after beam shut-off. Levels in the aisle along the accelerator vary from 0.1 mr/hr to over 1 R/hr, and decrease by an order of magnitude within the first eight hours.

Cooling water along the accelerator, and especially in the slits, collimators and beam dumps, will become radioactive. Typical levels in the water of a dump^{13,14} when irradiated to saturation with 1 MW beam power are shown in Table 2. It is apparent that this water presents a significant hazard to health, and must be carefully shielded and monitored. The radioactive water of each unit is contained within a closed loop, with non-radioactive water cooling in a heat exchanger outside the main earth shield. Water in the radioactive side of the loop will be monitored on a sampling basis, while the non-radioactive water will be monitored continuously for ruptures, etc., to ascertain that no significant amounts of radioactivity will reach the cooling tower, and thence, the outside world.

Radioactive and chemically active air produced inside the tunnel will present a significant hazard to personnel. Using a 3% beam power loss uniformly distributed along the accelerator, DeStaebler¹⁵ has calculated the rate of formation of noxious chemicals in the tunnel to be about 1 ppm/day. For radioactive air, the following reactions are of concern:¹⁶ $N^{14}(\gamma, n)N^{13}$, $N^{14}(n, 2n)N^{13}$, $O^{16}(\gamma, n)O^{15}$, with $A^{40}(\gamma, n)Cl^{39}$ and $N^{14}(\gamma, 2np)C^{11}$ also of importance. The equilibrium concentrations in the tunnel are shown in Table 3. From this it is calculated that if a person enters the tunnel immediately after beam shut-off, and remains for a period significantly long compared with the half-lives of the nuclides involved, he would receive a total exposure of 97 mrem from radioactive gas. A wait time of 20 minutes before entry would decrease this to 20 mrem. To reduce this hazard, the tunnel, which is normally sealed from the outside world, is first vented before entry is permitted. One complete air change occurs approximately every ten minutes.

Radioactive air has been monitored at the 660 foot accelerator, using a conventional Geiger tube and air pump arrangement. Beam conditions and target geometry are such that no correlation with calculation has been possible. Ozone is measured utilizing the chemiluminescence of ethylene gas in the presence of ozone. Air to be measured is mixed with a stream of ethylene gas near the face of a P.M. tube, and the resulting current measured with an electrometer. Response of this instrument is linear from 2×10^{-2} ppm to 3 ppm ozone. It is insensitive to nitrogen dioxide. A concentration of 2×10^{-2} ppm ozone gives a net signal equal to dark current (3×10^{-10} amps) with 1400 V applied to the P.M. tube, and 8 cc/min ethylene gas and 1300 cc/min air. Sensitivity may be increased by increasing ethylene gas flow rate and/or HV.

Ozone is produced in the tunnel from charged particles in the electromagnetic shower which get into the air.¹⁵ Again, beam, target and other conditions are such that we have not been able to correlate with calculations. We have measured, for 2.7 kW beam power absorbed, 1.5×10^{-5} μ c/cc radioactive air, and 0.1 ppm ozone concentration.

3. Radiation Not Associated with the Beam

The two mile accelerator will use 240 klystrons, each with a design power of 24 MW, to achieve a final electron energy of 20 BeV. 960 klystrons will be used for a design maximum electron energy of 40 BeV. The 250 kVp x-rays emitted from these tubes must be shielded and monitored. Shielding is accomplished by the iron focusing magnet, and 1/16 inch Pb sheet. Monitoring proved to be a difficult problem using conventional electrometer tube input ionization chambers. Modulator noise, and perhaps some rf leakage,

produced too much interference for any commercially available ionization counters except those with excessive iron shielding. The use of a MOS input stage to replace the electrometer tube, as reported by J. B. McCaslin,¹⁷ was found to satisfy our needs. SLAC has developed an ion chamber with MOS input and subsequent amplifier stages which is light, sensitive (2 mr/hr full scale on the most sensitive range using a 1/2 liter ion chamber), fast (two seconds time constant on the 2 mr/hr range), and completely insensitive to rf or noise pulses found at SLAC.

SUMMARY

Many of the original shielding calculations of DeStaebler have been checked, in particular the radiation through a thick shield, radiation streaming up a penetration, and so on. In addition, along with other experimenters, we have verified the giant resonance yield formula. In all cases we have found good agreement with theory. However, we wish to emphasize that many of our measurements have been preliminary in nature, using a machine that is constantly being tuned and altered, and about which we know little of the daily beam loss points, etc. Also, most of our measurements still lie ahead; i.e., skyshine measurements, neutron spectrum determinations, QF determinations, and so on. Most of these measurements will have to wait until completion of the machine, sometime in 1966.

ACKNOWLEDGEMENTS

We note our indebtedness to H. DeStaebler who made all the original shielding calculations at SLAC, which we are now in the process of verifying. We also wish to thank Walter R. Nelson for help on calculations and T. Ginn for aiding in many of the measurements.

REFERENCES

1. H. DeStaebler, Transverse Radiation Shielding for the Stanford Two-Mile Accelerator, USAEC Report SLAC Report No. 9, November 1962.
2. B. J. Moyer, University of California Lawrence Radiation Laboratory, Build-up Factors, in Conference on Shielding of High Energy Accelerators, New York, April 1957, USAEC Report TTD-7545, pp. 96-100, 1957.
3. K. G. Dedrick and H. H. Clark, Photoneutron Yields from Excitation of the Giant Resonance, Project M-225, Stanford University, September 1960.
4. W. C. Barber and W. D. George, Neutron Yields from Targets Bombarded by Electrons, Phys. Rev. 116, 1551 (December 15, 1959).
5. G. Bathow, E. Freytag and K. Tesch, Die Abschirmung von 4.8 GeV Bremsstrahlung durch Schwerbeton, German Report DESY 64/11.
6. H. DeStaebler, T. Jenkins, W. R. Nelson, Reduction of the Thermal Neutron Flux in Concrete Using Paraffin Moderators, USAEC Report SLAC TN 65-11, January 1965.
7. D. A. G. Neet, Radiation Exposure in the Switchyard, USAEC Report SLAC TN 65-9, January 1965.
8. H. DeStaebler, Radiation Problems Arising from Holes in the Transverse Shielding, USAEC Report SLAC TN 62-71, November 1962.
9. B. T. Price, C. C. Horton, K. T. Spinney, Radiation Shielding, Pergamon Press, New York, 1957.
10. H. DeStaebler, T. Jenkins, PuBe Neutron Measurements in the Accelerator Tunnel, USAEC Report SLAC TN 65-24, March 1965.
11. H. DeStaebler, Average Radiation Levels Inside the Accelerator Housing When the Machine Is Off, USAEC Report SLAC TN 62-70, October 1962.
12. H. DeStaebler, Photon-Induced Residual Activity Summary, USAEC Report SLAC TN 63-92, November 1963.
13. H. DeStaebler, Tritium Production in Water, USAEC Report SLAC TN 64-6, January 1964.
14. D. Coward, Stanford Linear Accelerator Center, private communication.
15. H. DeStaebler, Electron-Photon Flux in the Tunnel When the Machine Is On: Applications to Chemically Active Air and to Active Cooling Water, USAEC Report SLAC TN 62-80, December 1962.
16. H. DeStaebler, Radioactive Gas in the Tunnel, USAEC Report SLAC TN 62-9, March 1962.
17. J. B. McCaslin, Electrometer for Ionization Chambers Using Metal-Oxide Semiconductor Field-Effect Transistors, Rev. Sci. Instru. 35, (11), 1587-1591 (1964).

TABLE 1

PHOTON INDUCED ACTIVITIES IN COPPER

| Daughter Nuclide Element | A | Mean Life ³ τ (hr) | Radiation ($+$ \rightarrow β^+ , γ energy in MeV) | E_{γ} ³ (MeV) | Yield Relative ^{6,*} to Cu ⁶² | RE_{γ} (Energy) \times (Activity) ^{**} (MeV-curies) |
|--------------------------|----|--|--|------------------------------------|---|---|
| Cu | 64 | 18.4 | +,- | 0.60 | 0.58 | 390.0 |
| | 62 | 0.23 | $\sim 2\%$ γ , + | 1.10 | 1.00 | 1230.0 |
| | 61 | 4.8 | $\sim 10\%$ γ , + | 0.94 | 0.18 | 190.0 |
| Ni | 57 | 52.0 | 1.4,1.9,+ | 1.99 | 1.8×10^{-3} | 4.0 |
| Co | 60 | 6.6×10^4 | 1.17,1.33 | 2.51 | (2.0×10^{-2}) | 56.0 |
| | 58 | 2.8×10^2 | 0.80, + | 0.94 | (2.7×10^{-2}) | 28.0 |
| | 56 | 2.7×10^3 | .89,others,+ | 0.70 | (1.2×10^{-2}) | 9.4 |
| | 55 | 26.0 | many, + | 2.02 | 8.5×10^{-4} | 1.9 |
| Fe | 59 | 1.56×10^3 | 1.1,1.3 | 1.29 | (3.0×10^{-3}) | 4.3 |
| Mn | 56 | 3.7 | 0.8,2.8 | 1.80 | 3.0×10^{-3} | 6.1 |
| | 54 | 1.0×10^4 | 0.8 | 0.84 | (5.0×10^{-3}) | 4.7 |
| | 52 | 2.0×10^2 | 1.4, + | 2.45 | 1.3×10^{-3} | 3.6 |
| | 51 | 1.1 | + | 1.02 | (1.2×10^{-3}) | 1.4 |

* Parentheses indicate that yield is inferred, not measured.

** For a power absorption of 3% of 2.4 MW.

ACTIVITY IN COPPER INDUCED BY NEUTRONS

| Reaction | Mean Life τ (hr) | Radiation ($+$ \rightarrow β^+ , γ energy in MeV) | E_{γ} (MeV) | (Energy)(Activity) RE_{γ} (Curies-MeV) | $\frac{(RE_{\gamma})\gamma}{(RE_{\gamma})n}$ |
|---|-----------------------------|--|-----------------------|---|--|
| Cu ⁶⁵ (n,2n)Cu ⁶⁴ | 18.4 | +,- | 0.60 | 20.0 | 20 |
| (n,p)Ni ⁶⁵ | 3.7 | 1.1,1.4 | 0.59 | 2.8 | |
| (n, α)Co ⁶² | 0.34 | $\lesssim 1.2$ | ≈ 1.3 | | |
| Cu ⁶³ (n,2n)Cu ⁶² | 0.23 | $\sim 2\%$ γ , + | 1.10 | 80.0 | 15 |
| (n,p)Ni ⁶³ $\sim 10^6$ | | 0.0 | 0.0 | 0.0 | |
| (n, α)Co ⁶⁰ | 6.6×10^4 | 1.17,1.33 | 2.51 | | |

TABLE 2

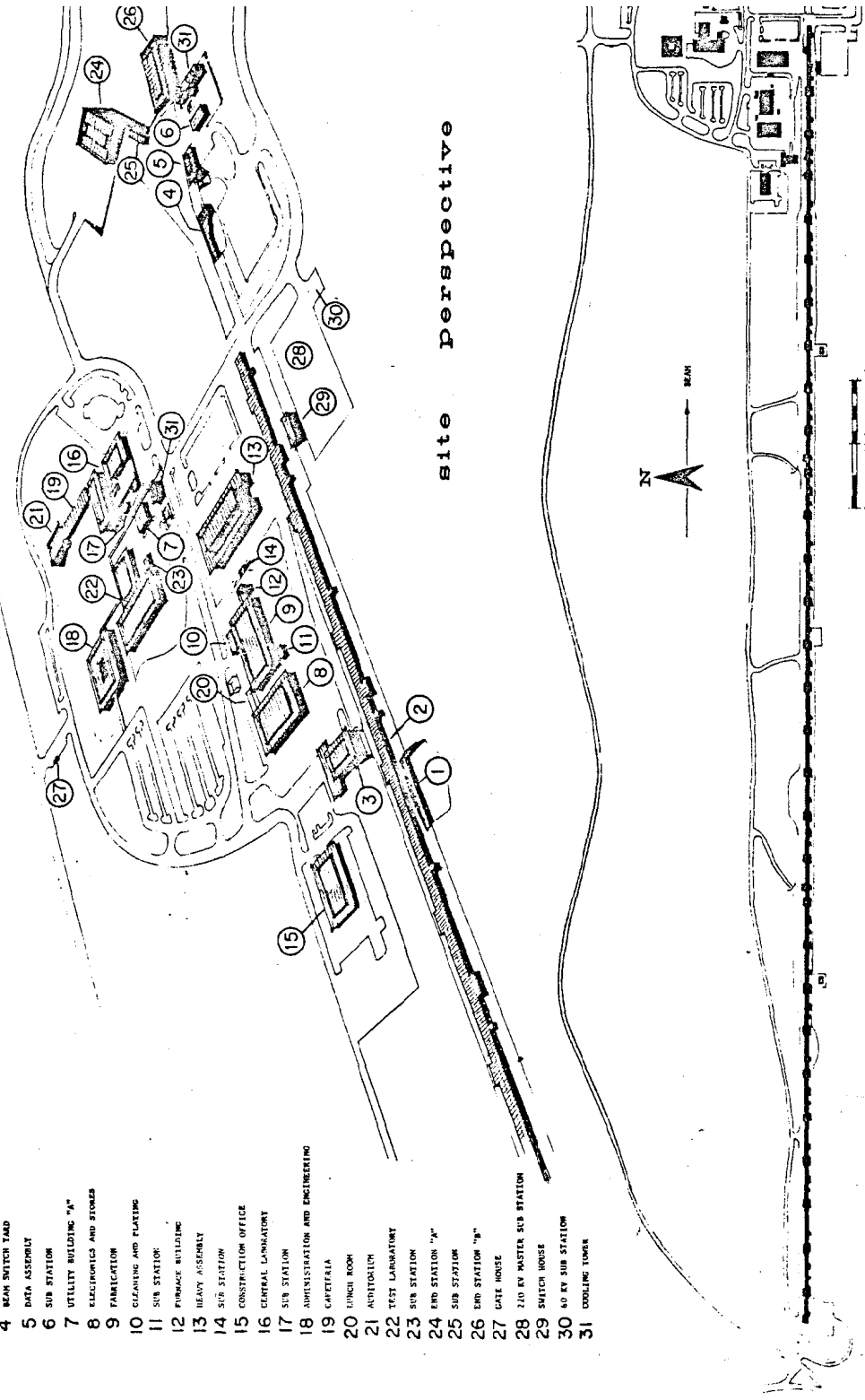
| <u>Daughter Nuclide</u> | <u>R (curies)</u> | <u>Mean Life τ (hours)</u> |
|-----------------------------|-------------------|--|
| O ¹⁵ | 35,000 | 0.05 |
| N ¹³ | 1,390 | 0.24 |
| C ¹¹ | 1,390 | 0.5 |
| Be ⁷ | 280 | 1.85×10^3 |
| H ³ | 400 | 1.55×10^5 |

TABLE 3

| <u>Final Nuclide</u> | | <u>Rate of Formation R (nuclides/sec)</u> | <u>Equilibrium Concentration in Tunnel ($\mu\mu$ curies/cm³)</u> |
|----------------------|-------------------|---|--|
| C ¹¹ | | 0.24×10^{10} | 3.1 |
| N ¹³ | incident γ | 12.0×10^{10} | |
| | incident n | $< 3.0 \times 10^{10}$ | |
| | total | 15.0×10^{10} | 190.0 |
| O ¹⁵ | | 17.0×10^{10} | 220.0 |
| Cl ³⁹ | | 0.42×10^{10} | 5.5 |

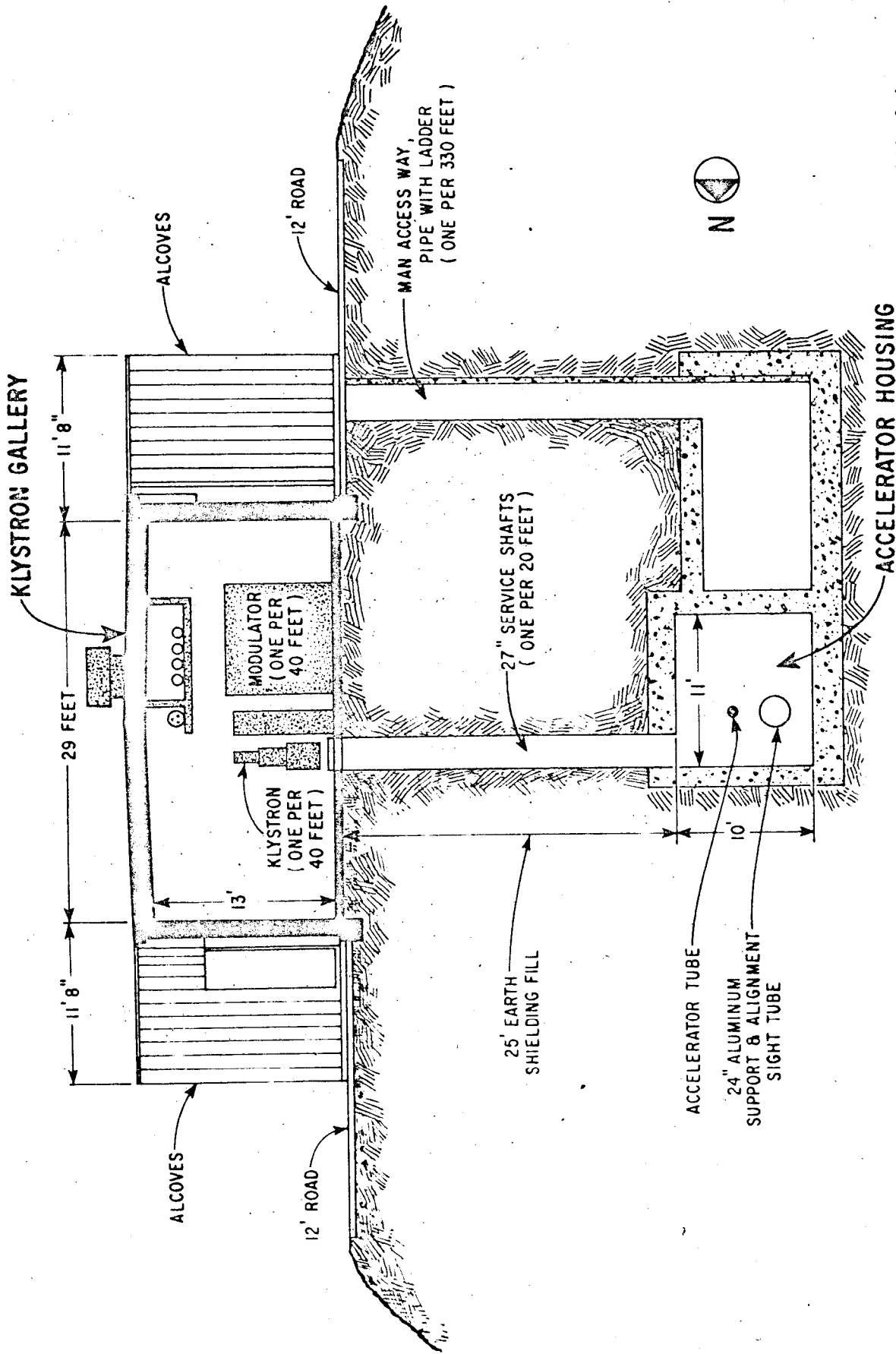
- 1 ACCELERATOR HOUSING
- 2 ELECTRON GALLERY
- 3 CONTROL BUILDING
- 4 BEAM SWITCH YARD
- 5 DATA ASSEMBLY
- 6 SUB STATION
- 7 UTILITY BUILDING "A"
- 8 ELECTRONICS AND STORES
- 9 FABRICATION
- 10 CLEANING AND PLATING
- 11 SUB STATION
- 12 FURNACE BUILDING
- 13 HEAVY ASSEMBLY
- 14 SUB STATION
- 15 CONSTRUCTION OFFICE
- 16 CENTRAL LABORATORY
- 17 SUB STATION
- 18 ADMINISTRATION AND ENGINEERING
- 19 CAPTIFELA
- 20 LUNCH ROOM
- 21 AUDITORIUM
- 22 TEST LABORATORY
- 23 SUB STATION
- 24 END STATION "A"
- 25 SUB STATION
- 26 END STATION "B"
- 27 GATE HOUSE
- 28 210 KV MASTER SUB STATION
- 29 SWITCH HOUSE
- 30 60 KV SUB STATION
- 31 COOLING TOWER

site perspective



STANFORD LINEAR ACCELERATOR CENTER

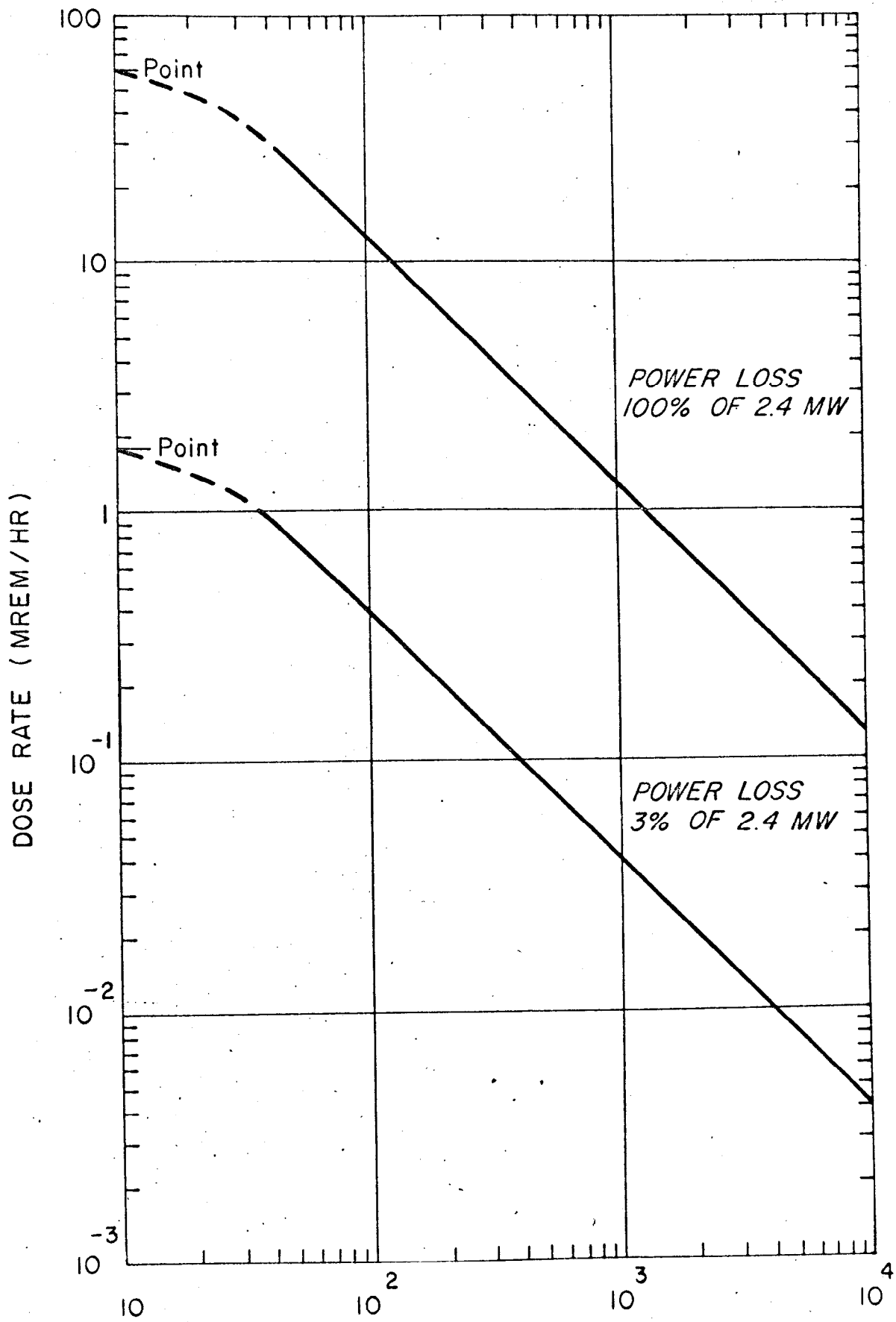
Fig. 1



283-12-A

ACCELERATOR CROSS SECTION
 LOOKING EAST IN DIRECTION OF BEAM

Fig. 2



ABSORPTION DISTANCE, l (Ft)
 Fig. 3

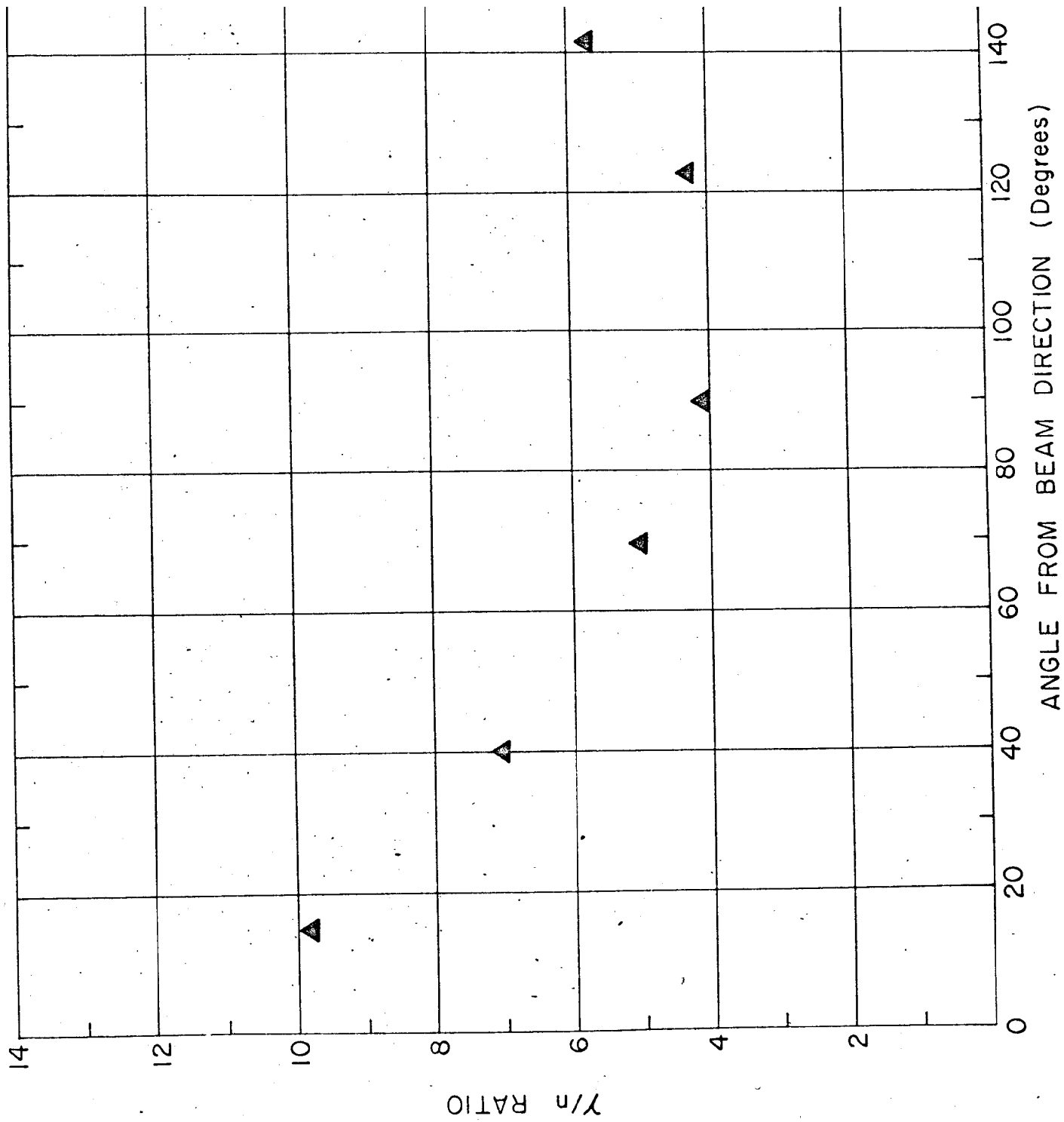


Fig. 4

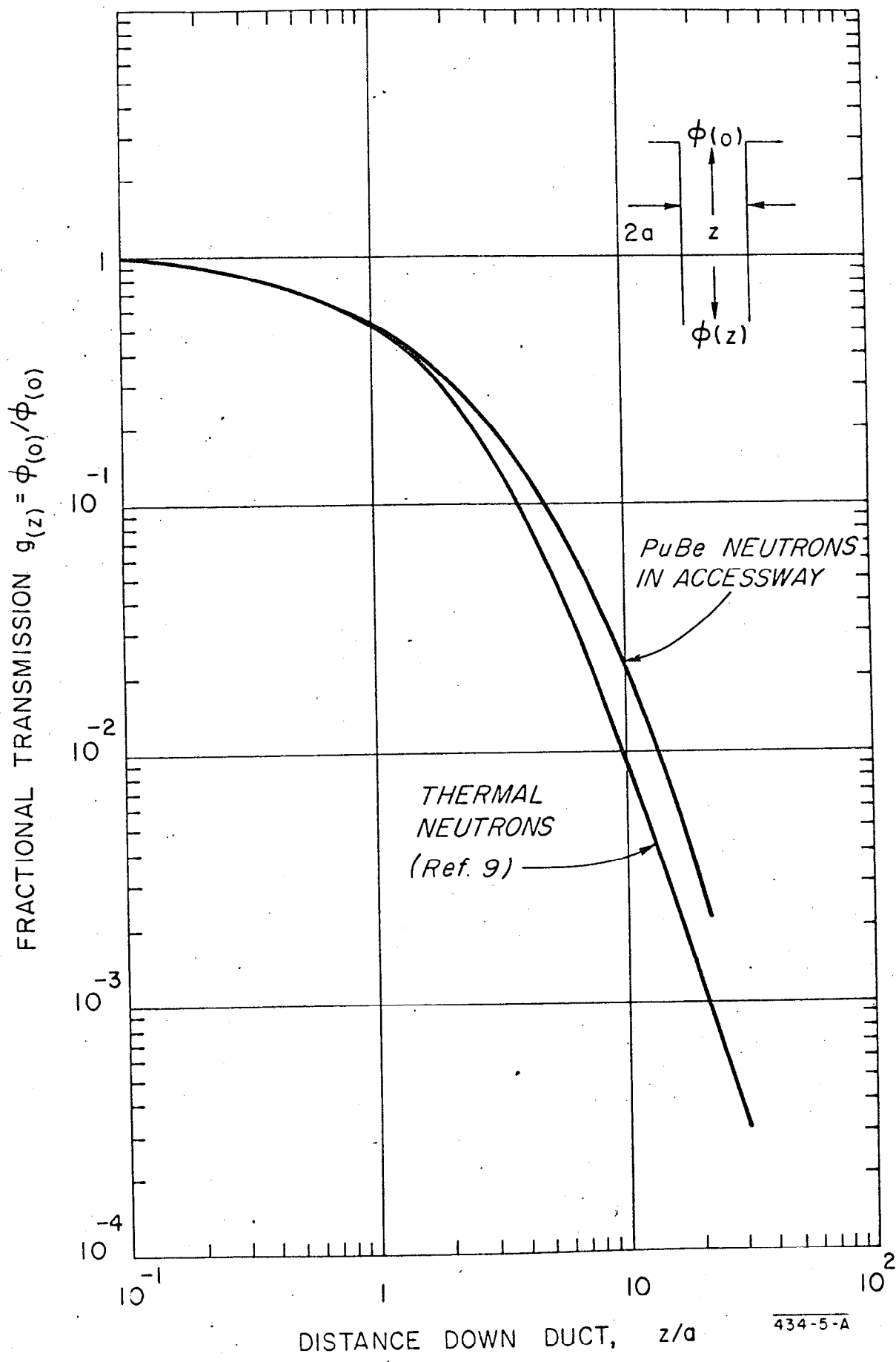


Fig. 5

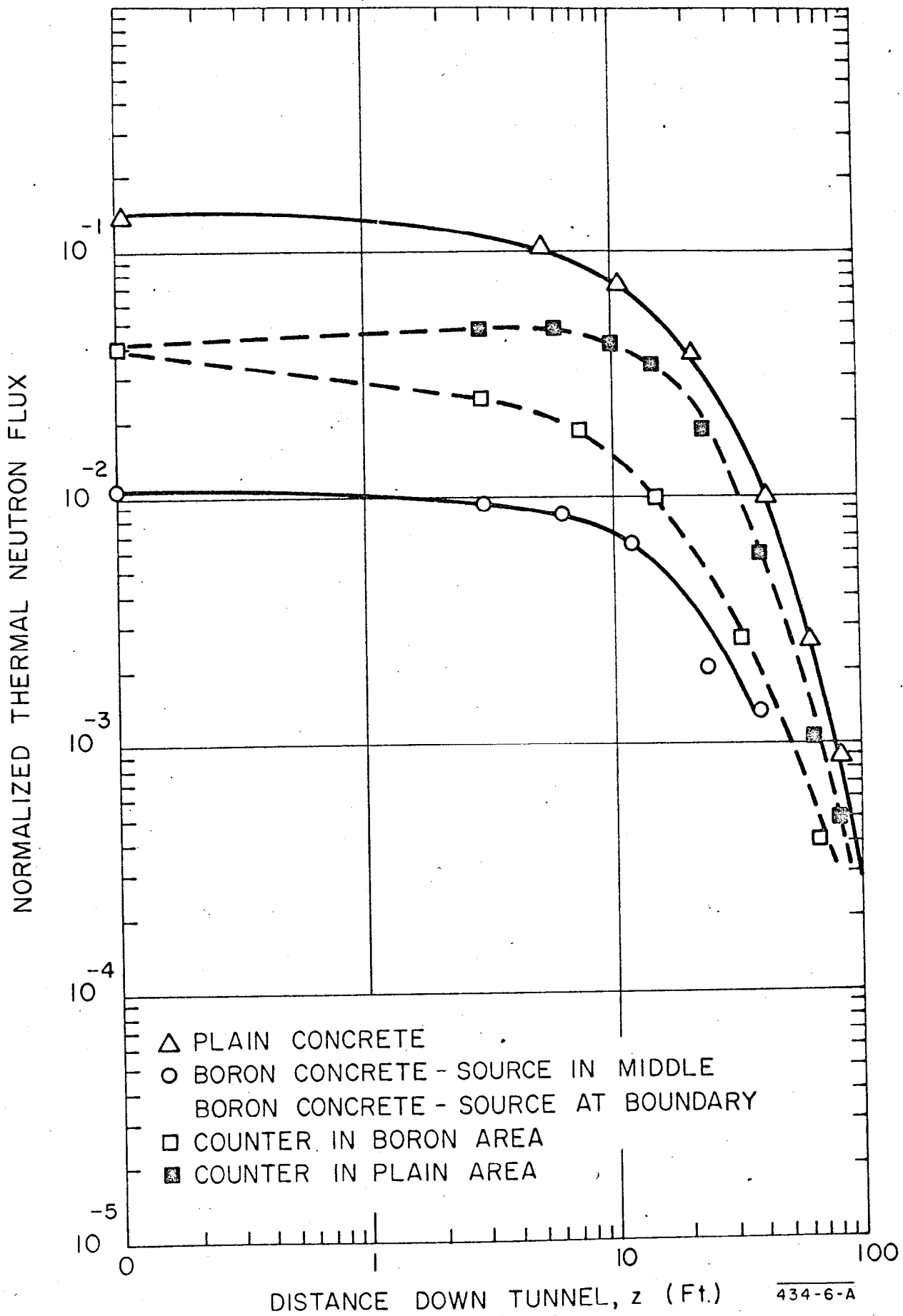


Fig. 6

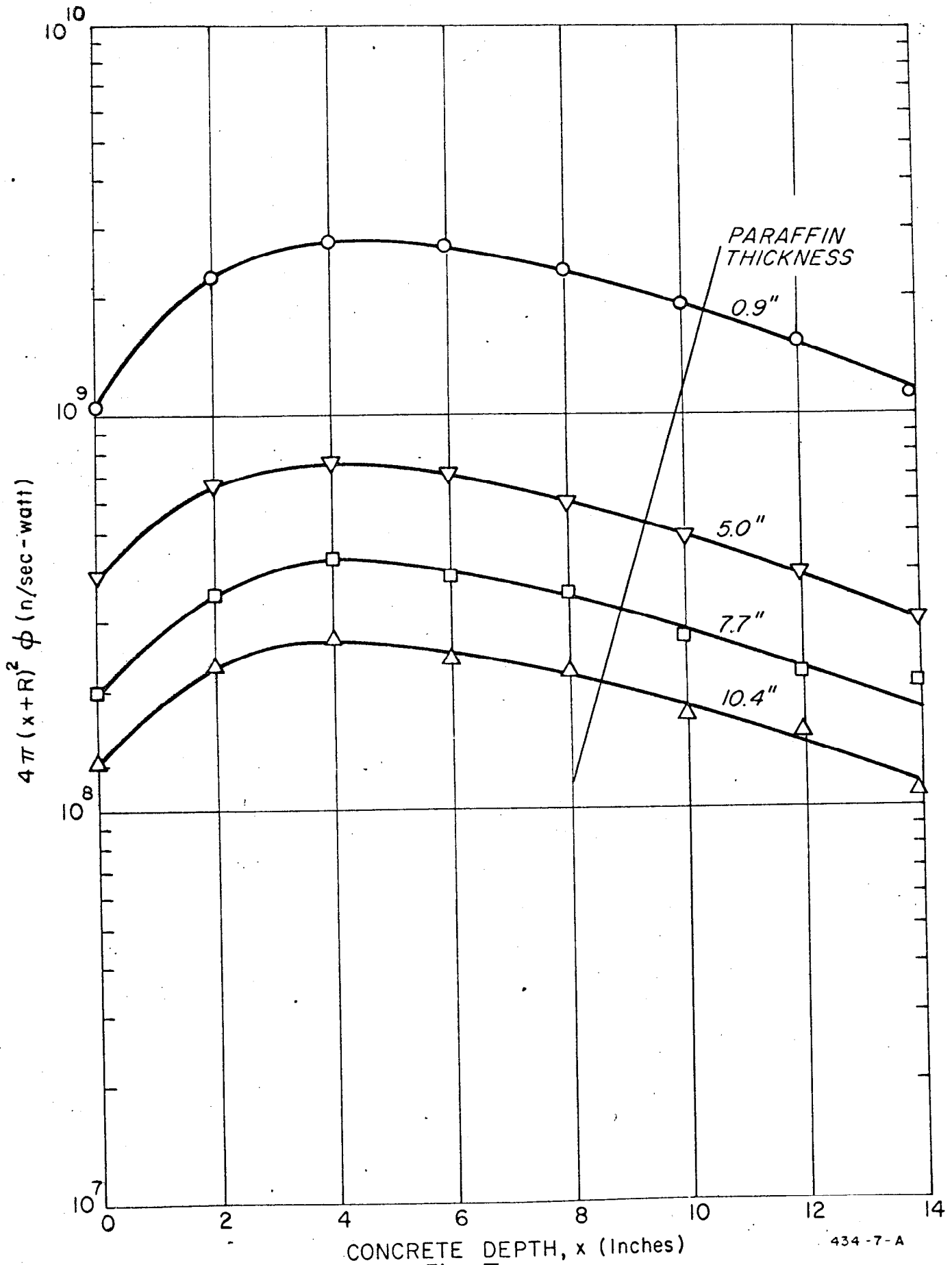
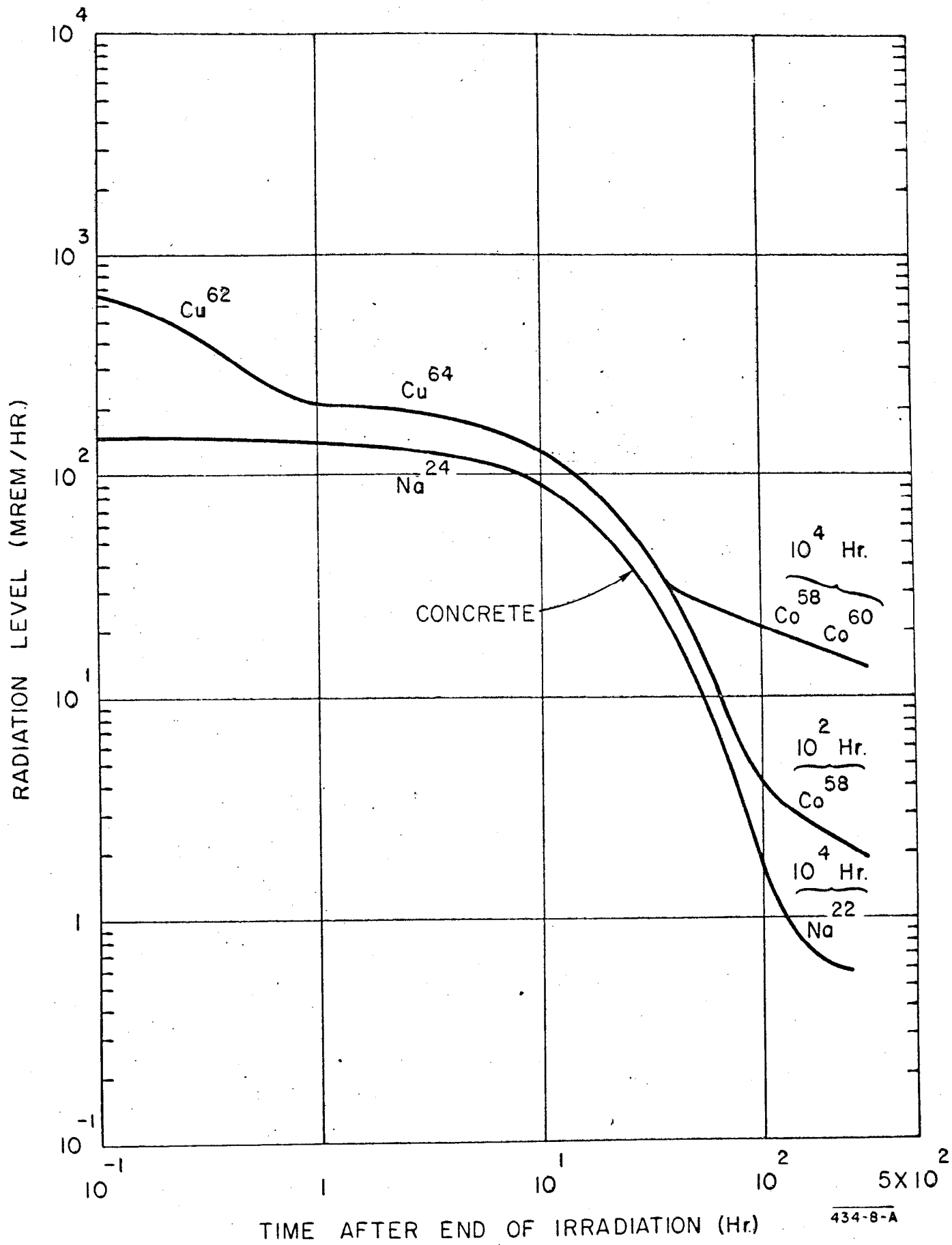


Fig. 7



TIME AFTER END OF IRRADIATION (Hr)

434-8-A

Fig. 8

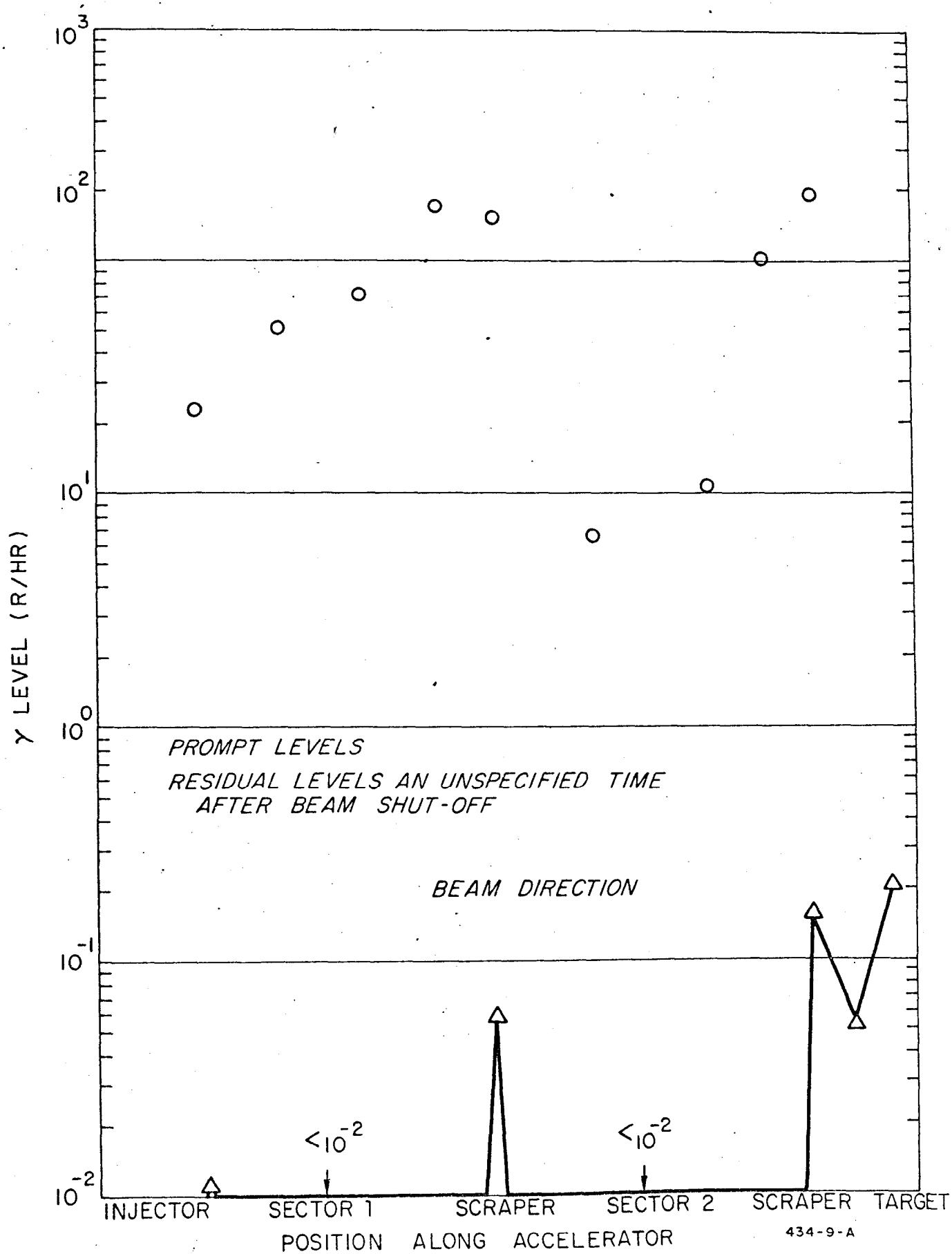


Fig. 9